AIAA JOURNAL
Vol. 31, No. 5, May 1993

Finite Element Modeling of Piezoelectric Sensors and Actuators

Woo-Seok Hwang* and Hyun Chul Park†
Pohang Institute of Science and Technology, Pohang 790-600, Republic of Korea

A finite element formulation for vibration control of a laminated plate with piezoelectric sensors/actuators is presented. Classical laminate theory with the induced strain actuation and Hamilton's principle are used to formulate the equations of motion. The total charge developed on the sensor layer is calculated from the direct piezoelectric equation. The equations of motion and the total charge are discretized with four-node, 12-degree-of-freedom quadrilateral plate bending elements with one electrical degree of freedom. The piezoelectric sensor is distributed, but is also integrated since the output voltage is dependent on the integrated strain rates over the sensor area. Also, the piezoelectric actuator induces the control moments at the ends of the actuator. Therefore, the number, size, and locations of the sensors/actuators are very important in the control system design. By selective assembling of the element matrices for each electrode, responses with various sensor/actuator geometries can be investigated. The static responses of a piezoelectric bimorph beam are calculated. For a laminated plate under the negative velocity feedback control, the direct time responses are calculated by the Newmark-β method, and the damped frequencies and modal damping ratios are derived by modal state space analysis.

Introduction

SPACE structures, aircraft, and the like are required to be light in weight due to the high cost of transportation. Since they are also lightly damped, owing to the low internal damping of the materials used in their construction, the increased flexibility may allow large amplitude vibration, which may cause structural instability. These problems lead to a drastic reduction in accuracy and precision of operation. Thus, it is highly desirable to control excessive vibration and to stabilize the structure during operation.[1-3]

Since structures are distributed parameter systems having an infinite set of vibration modes, distributed measurement and control is required. However, due to the limitations of materials and actuator design, the current design practice has involved the use of discrete sensors and actuators to control the vibration of distributed elastic systems. If the sensors are placed at nodal modes or lines of a vibration mode, that mode will be missed. These sensor/actuator (S/A) designs must also contend with the problems of control and observation spillover, which may destabilize the uncontrolled dynamics. Distributed sensors/actuators, which can detect and generate a number of vibration modes simultaneously and reduce the control spillover, are desirable to remedy the drawbacks of point S/As. An active control system, using distributed piezoelectric sensors and actuators, has proven to be effective in controlling the vibration of distributed elastic systems.[4-12]

Recent advances in design and manufacturing technologies have greatly enhanced the use of advanced fiber-reinforced composite materials for aircraft and aerospace structural applications. In addition to their high stiffness-to-weight ratio and strength-to-weight ratio, it is possible to control their structural properties by tailoring, which modifies the structural properties of the system without additional materials or mechanisms.[13,14] In structural control, the alteration of vibration modes with the change of stiffness and damping can affect performance. As a consequence, the integration of composite structural design with the intelligent system concept could potentially enhance the performance of aircraft and space structures. Numerous investigators have recently demonstrated the feasibility of the integrated concept. The use of lead zirconate titanate (PZT) ceramics and polyvinylidene fluoride (PVDF) thin film as a distributed active damper for beam vibration has been studied.[4-8] Elastic models for two-dimensional piezoelectric actuators bonded to the surface or embedded into the body of a beam have been developed.[9,10] Lee[11] and Lee et al.[12] developed a series of multimode piezoelectric S/As and performed the modal vibration control of a plate.

Several analyses and numerical models have been developed to analyze integrated structures. Most of them are based on analytic approaches[4-8,11,12] and the Ritz method.[9] Finite element methods for composite structures with integrated piezoelectric materials are described in Refs. 15-17. Therein the plate and the thin S/As are modeled with the isoparametric hexahedron solid element, which made the problem large and required some special techniques such as Guyan reduction to reduce the total degrees of freedom. Other problems associated with the isoparametric hexahedron solid element in thin continua analysis were the excessive shear strain energies and the higher stiffness coefficients in the thickness direction, as the thickness becomes very thin. To overcome these problems, three internal degrees of freedom were added in formulation, which made the problem large and complex.

The purpose of our research is to develop a more efficient finite element code for vibration control of a laminated composite plate with piezoelectric S/As attached to the structure element by modeling the mechanical-electrical response.

There are two essential ideas in this paper. The first is the development of a new piezoelectric plate element with one electrical degree of freedom. By modeling the plate and S/As with the new four-node, two-dimensional quadrilateral plate elements, the problems associated with solid element are eliminated and the problem size is much reduced, which saves much memory and computation time. The second is to develop a method for modeling the S/As of the various number and geometries of electrodes. The output voltage is dependent on the integrated strain rates over the electrode area of the sensor, which is called the integrated effect of the piezoelectric sensor. Also the piezoelectric actuator induces the control

Received June 4, 1992; revision received Sept. 14, 1992; accepted for publication Sept. 14, 1992.

*Research Assistant, Department of Mechanical Engineering. Member AIAA.

†Associate Professor, Department of Mechanical Engineering. Member AIAA.

moments at the ends of the actuator. Therefore, the number, size, and locations of S/As are very important in the control system design. By selective assembling of the element matrices for each electrode, responses with the various sensor and actuator geometries can be investigated. In implementing the piezoelectric S/A, since the voltage from the sensor or to the actuator is one definite value for each electrode, only one electrical degree of freedom for each element, not for each node, is enough to model the electrical response of an element. The problem of voltage assignment to the electrical degree of freedom for the common nodes can be overcome by the electrical degree of freedom for each element, when the different input voltages are applied to the adjacent actuators. Such effects of the number and geometries of electrodes will be shown in numerical examples. The static response of a piezoelectric bimorph beam to electrical loading and sensor voltage to the given displacement are calculated. The results are compared with experiments and solutions of previous studies.[15,16] For a laminated plate under the negative velocity feedback control, the direct time response by the Newmark-β method and damped frequencies and modal damping ratios with negative velocity feedback control by modal state space analysis are derived.

Derivation of Equations

Equations of Motion for a Laminated Plate

To derive the equation of motion for the laminated composite plate with sensor/actuator layers in Fig. 1, we used Hamilton's principle

$$\delta \int_{t_1}^{t_2} [T - U + W]\, \mathrm{d}t = 0 \tag{1}$$

where T is the kinetic energy, U the potential energy, and W the work done by the external forces. The S/A layer is treated as another layer with different material properties in deriving the kinetic energy and potential energy.

When only the response of flexural vibration is considered, inplane displacements are ignored. Therefore, the displacements and strains are expressed as follows:

$$\boldsymbol{u} = \begin{bmatrix} u_x \\ u_y \\ u_z \end{bmatrix} = \begin{bmatrix} -z\dfrac{\partial w}{\partial x} \\ -z\dfrac{\partial w}{\partial y} \\ w \end{bmatrix} = \begin{bmatrix} 0 & z & 0 \\ 0 & 0 & z \\ 1 & 0 & 0 \end{bmatrix} v \tag{2}$$

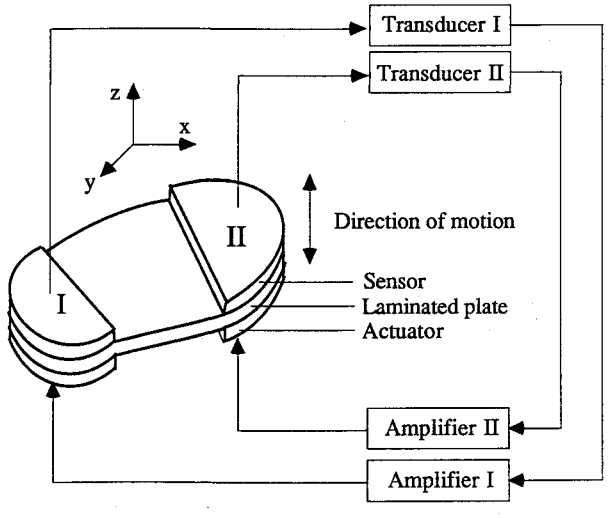

Fig. 1 Configuration of a laminated plate with piezoelectric sensor/actuator.

$$\epsilon = \begin{bmatrix} \epsilon_x \\ \epsilon_y \\ \gamma_{xy} \end{bmatrix} = \begin{bmatrix} z\dfrac{\partial \beta_x}{\partial x} \\ z\dfrac{\partial \beta_y}{\partial y} \\ z\dfrac{\partial \beta_y}{\partial x} + z\dfrac{\partial \beta_x}{\partial y} \end{bmatrix} = z\kappa \tag{3}$$

where $v = \{w \;\; \beta_x \;\; \beta_y\}^T$, w is the normal displacement, and $\beta_x (= -\partial w/\partial x)$ and $\beta_y (= -\partial w/\partial y)$ are the rotations of the normal to the undeformed middle surface in the x-z and y-z planes, respectively. The kinetic energy T is defined as

$$T = \int_V \tfrac{1}{2}\rho \dot{\boldsymbol{u}}^T \dot{\boldsymbol{u}}\, \mathrm{d}V = \int_A \tfrac{1}{2} \dot{v}^T \boldsymbol{R} \dot{v}\, \mathrm{d}A \tag{4}$$

where $\boldsymbol{R}$ is the inertia matrix, i.e., diag $\{t \;\; t^3/12 \;\; t^3/12\}$ with t the thickness of the plate. The strain energy of each layer is[18]

$$U_k = \frac{1}{2} \int_{V_k} \{\epsilon_1 \; \epsilon_2 \; \gamma_{12}\} \begin{bmatrix} \sigma_1 \\ \sigma_2 \\ \tau_{12} \end{bmatrix} \mathrm{d}V_k \tag{5}$$

where V_k is the volume and U_k the strain energy of the kth layer. Transforming the stresses and strains in principal material coordinates to those in the directions of the plate major axes, we have

$$U_k = \frac{1}{2} \int_{V_k} \epsilon^T \bar{\boldsymbol{Q}}\, \epsilon\, \mathrm{d}V_k \tag{6}$$

where the transformed reduced stiffnesses $\bar{\boldsymbol{Q}}$ are given in terms of the reduced stiffness $\boldsymbol{Q}$ and the layer angle by

$$\bar{\boldsymbol{Q}} = \boldsymbol{P}^{-1}\, \boldsymbol{Q}\, \boldsymbol{P} \tag{7}$$

where $\boldsymbol{P}$ is the transformation matrix. If the strain components in Eq. (3) are substituted into Eq. (6), and the potential energy for each layer is summed up in the z direction, the total strain energy U is

$$U = \frac{1}{2} \int_A \kappa^T \boldsymbol{D}\, \kappa\, \mathrm{d}A \tag{8}$$

where $\boldsymbol{D}$ is the flexural stiffness of an anisotropic plate

$$D_{ij} = \frac{1}{3} \sum_{k=1}^{N} (\bar{Q}_{ij})_k\, (z_k^3 - z_{k-1}^3) \tag{9}$$

The work by external forces f is

$$W = \int_A v^T f\, \mathrm{d}A \tag{10}$$

Piezoelectric Equation

The linear piezoelectric coupling between the elastic field and the electric field can be expressed by the direct and the converse piezoelectric equations, respectively.[19] These equations for a plate shape sensor and actuator are written as follows:

$$\begin{bmatrix} B_x \\ B_y \\ B_z \end{bmatrix} = \begin{bmatrix} e_{11} & e_{12} & e_{16} \\ e_{21} & e_{22} & e_{26} \\ e_{31} & e_{32} & e_{36} \end{bmatrix} \begin{bmatrix} \epsilon_x \\ \epsilon_y \\ \gamma_{xy} \end{bmatrix} + \begin{bmatrix} \epsilon_{11}^s & \epsilon_{12}^s & \epsilon_{13}^s \\ \epsilon_{21}^s & \epsilon_{22}^s & \epsilon_{23}^s \\ \epsilon_{31}^s & \epsilon_{32}^s & \epsilon_{33}^s \end{bmatrix} \begin{bmatrix} E_x \\ E_y \\ E_z \end{bmatrix} \tag{11}$$

$$\begin{bmatrix} \sigma_x \\ \sigma_y \\ \tau_{xy} \end{bmatrix} = \begin{bmatrix} c_{11} & c_{12} & c_{16} \\ c_{12} & c_{22} & c_{26} \\ c_{16} & c_{26} & c_{66} \end{bmatrix} \begin{bmatrix} \epsilon_x \\ \epsilon_y \\ \gamma_{xy} \end{bmatrix} - \begin{bmatrix} e_{11} & e_{21} & e_{31} \\ e_{12} & e_{22} & e_{32} \\ e_{16} & e_{26} & e_{36} \end{bmatrix} \begin{bmatrix} E_x \\ E_y \\ E_z \end{bmatrix} \tag{12}$$

where $\boldsymbol{B}$ is the electric displacement vector (charge/area), $\boldsymbol{E}$ the electric field (volt/length), $\boldsymbol{e}$ the piezoelectric coefficient, ϵ^s the dielectric constant, and $\boldsymbol{c}$ the compliance matrix.

Sensor Equation

The direct piezoelectric equation (11) is used to calculate the output charge created by the strains in the plate.[11,12] Since no external electric field is applied to the sensor layer, the electric displacement developed on the sensor surface is directly proportional to the strain acting on the sensor. If the poling direction is z for sensors with the electrodes on the upper and lower surfaces, the electric displacement is derived from Eq. (11) as

$$B_z = e_{31}\,\epsilon_x + e_{32}\,\epsilon_y + e_{36}\,\gamma_{xy} \tag{13}$$

The total charge $q(t)$ developed on the sensor surface is the spatial summation of all point charges developed on the sensor layer. Hence, we have

$$q(t) = \int_y \int_x (e_{31}\,\epsilon_x + e_{32}\,\epsilon_y + e_{36}\,\gamma_{xy})\,dx\,dy \tag{14}$$

When piezoelectric sensors are used as strain rate sensors, the output charge can be transformed to sensor voltage as follows. The current on the surface of a sensor can be expressed as

$$i(t) = \frac{dq(t)}{dt} \tag{15}$$

The current is converted into the open circuit sensor voltage output V^s by

$$V^s(t) = G^C\,i(t) = G^C\,\frac{dq(t)}{dt} \tag{16}$$

where G^C is the gain of the current amplifier.

Actuator Equation

The actuator equations for two-dimensional piezoelectric actuator are derived from classical laminate theory with induced strain actuation.[9-12] The inplane actuator strain can be derived from the converse piezoelectric equation in Eq. (12). Since no stress field is applied to the actuator layer, the strains developed by the electric field on the actuator layer are given by

$$\epsilon^A = \boldsymbol{c}^{-1}\,\boldsymbol{e}^T\,\boldsymbol{E} = \boldsymbol{d}\,\boldsymbol{E} \tag{17}$$

The stress-strain relation for an actuator layer can be expressed as

$$\sigma = \bar{\boldsymbol{Q}}\epsilon \tag{18}$$

The resultant moments acting on a laminate are obtained by integrating stresses in each layer or lamina through the laminate thickness. The equivalent actuator moments $\boldsymbol{M}^A$ per unit length can be found by substituting Eq. (17) into Eq. (18) and integrating it through the thickness of the plate

$$\boldsymbol{M}^A = \int_t \bar{\boldsymbol{Q}}\epsilon^A z\,dz \tag{19}$$

When the voltage V^A with actuator thickness t^A is applied in the thickness direction only, the electric fields are

$$\boldsymbol{E} = [0\ \ 0\ \ V^A/t^A]^T \tag{20}$$

Substituting Eq. (20) into Eq. (19) results in the equivalent actuator moments $\boldsymbol{M}^A$ per unit length as a function of V^A

$$\boldsymbol{M}^A = \boldsymbol{L}\,V^A \tag{21}$$

where

$$L_i = \bar{Q}_{ij}\,d_{3j}\,\bar{z} \tag{22}$$

and $\bar{z}$ is the z coordinate of the middle plane of the piezoelectric material and the $L_i = 0$ outside the region where the actuator functions.

Finite Element Discretization

Plate Element with Electrical Degree of Freedom

The discrete Kirchhoff quadrilateral (DKQ) element in Fig. 2 is a four-node, 12-degree-of-freedom quadrilateral element for thin plates, derived using the so-called discrete Kirchhoff technique. The nodal variable $\boldsymbol{r}^e$ is defined as

$$\boldsymbol{r}^e = \{w_1\ \theta_{x1}\ \theta_{y1}\ w_2\ \theta_{x2}\ \theta_{y2}\ w_3\ \theta_{x3}\ \theta_{y3}\ w_4\ \theta_{x4}\ \theta_{y4}\}^T \tag{23}$$

where w is the normal displacement, $\theta_x\ (= \partial w/\partial y)$ and $\theta_y (= -\partial w/\partial x)$ are the rotation about the x and y axes. The displacement vector $v = \{w\ \ \beta_x\ \ \beta_y\}^T$ is expressed in nodal variables by finite element interpolation functions as follows:

$$\begin{bmatrix} w \\ \beta_x \\ \beta_y \end{bmatrix} = \begin{bmatrix} N(\xi,\eta) \\ H^x(\xi,\eta) \\ H^y(\xi,\eta) \end{bmatrix} \boldsymbol{r}^e \tag{24}$$

where N, H^X, and H^y are the interpolation functions for w, β_x and β_y, respectively.[20] Since the voltage is constant over an electrode, the number of electrical degree of freedom is one for each element. The electrical degree of freedom is used as a sensor voltage or actuator voltage when the piezoelectric material attached on a plate element behaves as a sensor or actuator.

Equations of Motion

Substituting energy terms into Eq. (1) yields the variational equation. To derive the discrete equations of motion for the system, the displacement v and the curvature κ are expressed in terms of nodal variables via the shape functions using the four-node, 12-degree-of-freedom quadrilateral plate bending element with one electrical degree of freedom as follows[20,21]:

$$v = \Psi_u\,\boldsymbol{r}^e \tag{25}$$

$$\kappa = \Psi_\kappa\,\boldsymbol{r}^e \tag{26}$$

where Ψ_u and Ψ_κ are the interpolation functions for v and κ, respectively. By substituting the discretized expression for displacements and curvature into the variational equation and assembling for the entire system, the equations of motion are expressed in terms of nodal variables

$$(\boldsymbol{M}_S + \boldsymbol{M}_P)\ddot{\boldsymbol{r}} + (\boldsymbol{K}_S + \boldsymbol{K}_P)\,\boldsymbol{r} = \boldsymbol{F}_{\text{ext}} \tag{27}$$

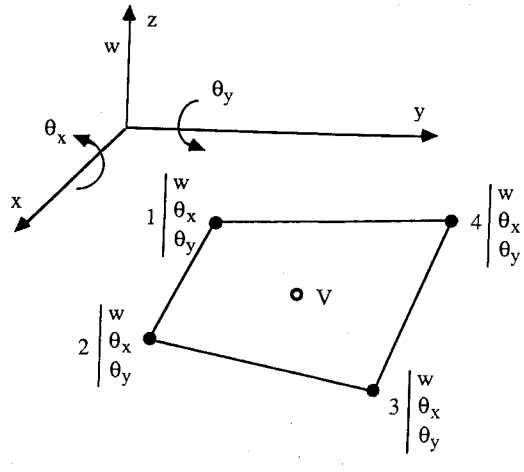

Fig. 2 Plate bending element with electrical degree of freedom.

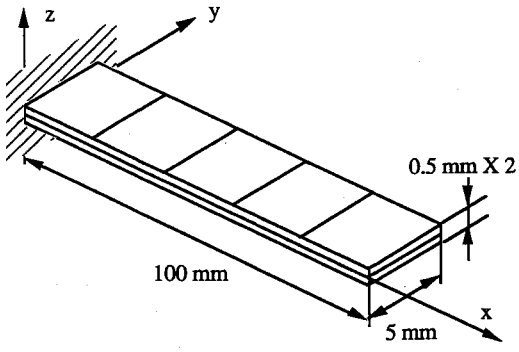

Fig. 3 Piezoelectric polymeric PVDF bimorph beam.

where

$$M_S = \sum_{\text{elem}} \int_{-1}^{1}\int_{-1}^{1} \Psi_u^T R_S \Psi_u |J| \, d\xi d\eta \tag{28a}$$

$$M_P = \sum_{\text{elem}} \int_{-1}^{1}\int_{-1}^{1} \Psi_u^T R_P \Psi_u |J| \, d\xi d\eta \tag{28b}$$

$$K_S = \sum_{\text{elem}} \int_{-1}^{1}\int_{-1}^{1} \Psi_\kappa^T D_S \Psi_\kappa |J| \, d\xi d\eta \tag{28c}$$

$$K_P = \sum_{\text{elem}} \int_{-1}^{1}\int_{-1}^{1} \Psi_k^T D_P \Psi_k |J| \, d\xi d\eta \tag{28d}$$

$$F_{\text{ext}} = \sum_{\text{elem}} \int_{-1}^{1}\int_{-1}^{1} \Psi_u^T f |J| \, d\xi d\eta \tag{28e}$$

and J is the Jacobian matrix. The subscripts S and P represent the main structure and the piezoelectric materials, respectively.

Sensor Equation

The total charge from the electrode of the jth sensor can be written by substituting Eq. (3) into Eq. (14)

$$q_j(t) = \int_{A_j^s} [e_{31}(z\kappa_x) + e_{32}(z\kappa_y) + e_{36}(z\kappa_{xy})] \, dA$$
$$= \bar{z} \int_{A_j^s} e\kappa \, dA \tag{29}$$

To express the total charge by nodal variables, substitute Eq. (26) into Eq. (29), yielding

$$q_j(t) = \Theta_j r \tag{30}$$

where

$$\Theta_j = \sum_{\text{elem}} \bar{z} \int_{-1}^{1}\int_{-1}^{1} e\Psi_\kappa |J| \, d\xi d\eta$$

and the element matrix is assembled only if that element is included in the jth sensor, i.e., the identity number of the electrode is j. Therefore, the jth sensor voltage V_j^s can be rewritten as

$$V_j^s = G_j^C \Theta_j \dot{r} \tag{31}$$

Actuator Equation

When the work W_{ctrl} done by active control forces due to m actuators is introduced in the Hamiltonian of Eq. (1), it can be seen as

$$W_{\text{ctrl}} = \sum_j^m \int_{A_j^A} \kappa^T M_j^A \, dA = \sum_j^m \int_{A_j^A} \kappa^T L \, dA \, V_j^A \tag{32}$$

If the variation of W_{ctrl} for nodal displacement is taken after Eq. (26) is substituted into Eq. (32), the control force by jth actuator is derived as follows:

$$F_{\text{ctrl}_j} = \int_{A_j^A} \Psi_\kappa^T L \, dA \, V_j^A = \Xi_j V_j^A \tag{33}$$

where

$$\Xi_j = \sum_{\text{elem}} \int_{-1}^{1}\int_{-1}^{1} \Psi_\kappa^T L |J| \, d\xi d\eta$$

and the element matrix is assembled only if that element is included in the jth actuator, i.e., the identity number of the electrode is j. The control forces in Eq. (33) are added to the equations of motion in Eq. (27).

Methods of Solution for Vibration Control

Direct Time Integration Method

The response of the system to given initial displacements or external loads in the time domain can be obtained by direct time integration of the equations of motion,[22] using the Newmark-β method. Increasing the time by Δt, the displacements, velocities, and accelerations are obtained from those of the previous step. Substituting the velocities into the sensor equation, output voltages are obtained. The input voltage to each actuator is calculated by multiplying the feedback gain G to the sensor voltage, and the control forces derived for the feedback voltage replace the previous control forces. These steps are repeated until the final time is reached.

State Space Equation of Motion with Feedback Control Law

The structural eigenvalue problem associated with the harmonic solutions for the undamped free vibration is

$$[-\omega^2(M_S + M_P) + (K_S + K_P)]\{\phi\} = 0 \tag{34}$$

where ω is the frequency of natural vibration and $\{\phi\}$ the mode shape. Using the orthogonality of the eigenvectors with respect to the mass matrix and the stiffness matrix, modal coordinates are introduced as follows:

$$r = \Phi\eta \tag{35}$$

where Φ is the modal matrix. When the modal state variable $x = \text{col}\{\eta \ \dot{\eta}\}$ is introduced, the modal state space equations of motion with control forces are as follows:

$$\dot{x} = Ax + Bu \tag{36}$$

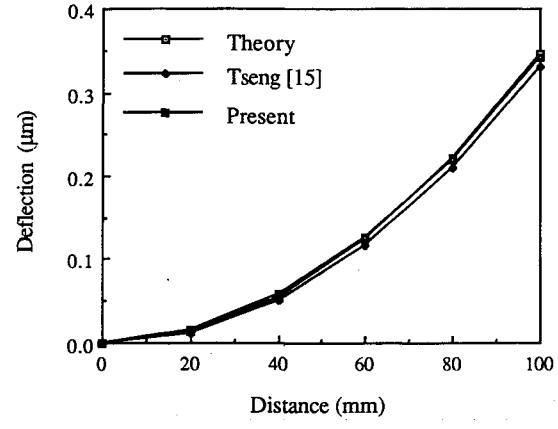

Fig. 4 Deflection of the piezoelectric PVDF bimorph beam (input voltage = 1 V).

where

$$A = \begin{bmatrix} \mathbf{0} & I \\ -[\omega^2] & -C_{\text{mod}} \end{bmatrix}$$

$$B = \begin{bmatrix} \mathbf{0} & \mathbf{0} & \dots & \mathbf{0} \\ \Phi^T \Xi_1 & \Phi^T \Xi_2 & \dots & \Phi^T \Xi_m \end{bmatrix}$$

$$u = [V_1^A \;\; V_2^A \;\; \dots \;\; V_m^A]^T$$

and m is the number of S/A. The modal structural damping matrix C_{mod} is derived from the definition of specific damping capacity in Adams[23] (see Appendix). The sensor equation in modal state space is

$$y = Cx \tag{37}$$

where

$$y = [V_1^s \;\; V_2^s \;\; \dots \;\; V_m^s]^T$$

$$C = \begin{bmatrix} \mathbf{0} & \mathbf{0} & \dots & \mathbf{0} \\ (G_1^C \Theta_1 \Phi)^T & (G_2^C \Theta_2 \Phi)^T & \dots & (G_m^C \Theta_m \Phi)^T \end{bmatrix}$$

If negative velocity feedback control is applied, the sensor voltage is multiplied by feedback gain and fed to the actuator. The linear feedback control law is

$$u = Gy = GCx \tag{38}$$

Complex Eigensolution Method

When the feedback control law in Eq. (38) is inserted into Eq. (36), the modal state space equations of motion are as follows:

$$\begin{aligned} \dot{x} &= Ax + Bu \\ &= Ax + BGCx \\ &= (A + BGC)x \end{aligned} \tag{39}$$

This can be analyzed as a complex eigenvalue problem,

$$[\lambda I - (A + BGC)]\{\phi\} = 0 \tag{40}$$

and the complex eigenvalue is

$$\lambda = \sigma + i\omega_d \tag{41}$$

Two measures of dynamic stability are the real part of the complex eigenvalue and the damping ratio. The imaginary part is 2π times the damped frequency, and the damping ratio

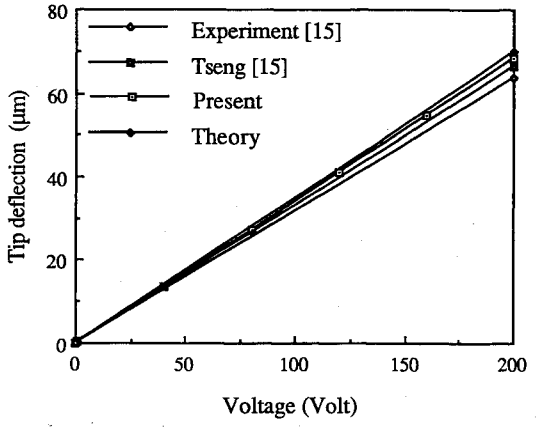

Fig. 5 Tip deflection of the piezoelectric PVDF bimorph beam vs input voltage.

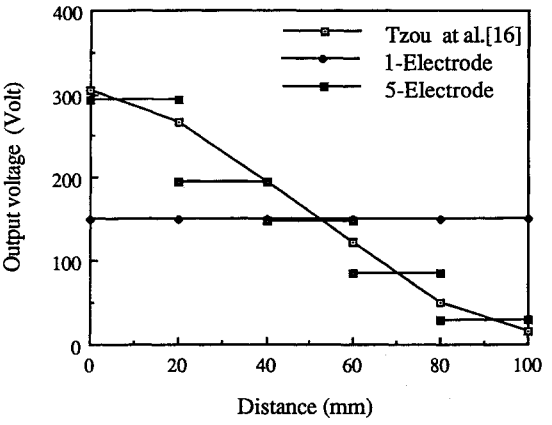

Fig. 6 Sensor voltage distribution for the bending deflection.

is defined to be the negative of the normalized real part of the complex eigenvalue.

$$f_d = \omega_d / 2\pi \qquad \zeta = -\sigma / \sqrt{\sigma^2 + \omega_d^2} \tag{42}$$

Numerical Examples

In this section, distributed sensing/actuation and vibration control are studied in two cases. The first case is a bimorph piezoelectric beam, which consists of two identical PVDF uniaxial beams with opposite polarities. And the second case is a plate composed of laminated composite whose stacking sequence is $[\pm\theta/0_2]_s$, with piezoelectric S/A pairs.

Piezoelectric Bimorph Beam

The bimorph piezoelectric beam,[15,16] which consists of two identical PVDF uniaxial beams with opposite polarities, is shown in Fig. 3. This cantilever beam is modeled with five identical plate elements, each element has the dimension of $20 \times 5 \times 1$ mm. The material properties of PVDF are shown in Table 1.

When the given external voltage is applied, the induced strain generates control forces that bend the bimorph beam. A unit voltage (1 V) is applied across the thickness and the static deflections at the nodes are calculated by the finite element method. The deflection of the beam is calculated for various applied voltages between 0 and 200 V. The calculated deflections are compared with those in the work of Tseng,[15] shown in Figs. 4 and 5, with good agreement. The total number of degrees of freedom used in this analysis is compared in Table 2 with that in Tseng's, showing that our finite element formulation with plate elements saves much memory and computation time.

The piezoelectric bimorph beam is also studied for sensing deflections. When the bimorph beam is used as a strain sensor, the open circuit voltage output V_j^S from the jth sensor layer is given by

$$V_j^S = q_j / C \tag{43}$$

where $C = \epsilon_0 S / t^S$, ϵ_0 is the absolute permittivity, S the area of electrode, and t^S the thickness of the sensor. The sensor voltage can be calculated by dividing the charges in Eq. (30) by C for each electrode.

When external tip loads (which produce the tip deflection of 1 cm) are applied, the output voltage is calculated using the finite element code we developed. In Tzou and Tseng's work,[16] the integrated effect of the piezoelectric sensor is neglected, which resulted in continuous voltage output along the beam length, although measuring such a voltage distribution on the electrode is impossible in reality. In this paper, two models of the sensor electrodes are used: the first is one for the whole beam and the second is an electrode for each element, i.e., five identical electrodes along the beam. The results are

Table 1 Material properties of composite materials and piezoelectric materials

Graphite/Epoxy			PZT		PVDF	
E_1	98 E9 N/m^2	s_{11}	16.4 E-12 m^2/N	E_1	2.0 E9 N/m^2
E_2	7.9 E9 N/m^2	s_{12}	−5.7 E-12 m^2/N	E_2	2.0 E9 N/m^2
G_{12}	5.6 E9 N/m^2	s_{33}	18.8 E-12 m^2/N	G_{12}	7.75 E8 N/m^2
t	0.125 E-3 m	s_{55}	47.5 E-12 m^2/N	t	0.5 E-3 m
ν_{12}	0.28	d_{31}	−171 E-12 C/N[b]	ν	0.29
ρ	1520 kg/m^3	d_{33}	374 E-12 C/N	ρ	1800 kg/m^3
φ_1	0.0045	d_{15}	584 E-12 C/N	d_{31}	2.2 E-11 C/N
φ_2	0.0420	ϵ_{11}/ϵ_0[a]	1730	ϵ_{11}	1.062 E-10 F/m[c]
φ_{12}	0.0706	ϵ_{33}/ϵ_0	1700	ϵ_{33}	1.062 E-10 F/m
		ρ	7700 kg/m^3	ϵ_{33}	1.062 E-10 F/m

[a]Here ϵ_0 is the permittivity of free space [$\epsilon_0 = 1/(36\pi \times 10^9)$ F m^{-1}].
[b]C/N ≡ Coulomb/Newton.
[c]F/m ≡ Farad/meter.

Table 2 Comparison of problem size and computation time

Method	Node no.	No. D.O.F Structure	Electrical	Total	$n^3/3$[a]
Tseng[15]	36	108	36	144	419,904
Present	12	36	5	41	15,552
Ratio, %[b]	33.3	33.3	13.9	28.5	3.7

[a]Computation time is dependent on the operation number $n^3/3$ when a linear matrix equation of order n is solved by LU method.
[b]Ratio = (quantity in present low)/(quantity in Tseng low).

compared with those of Tzou and Tseng[16] in Fig. 6. The sensor voltage for beam bending is dependent on the first derivative of the bending strain, i.e., the second derivative of flexural displacement.[10] The normalized theoretical second derivative of flexural displacement for bending of the cantilever beam and the sensor voltages are compared in Fig. 7. When the output voltage at five electrodes of the plate model with five elements (5 × 1) and with ten elements (10 × 1) are compared, the latter gives good agreement with the theoretical second derivative of flexural displacement. Because of the convergence of finite element solutions with finer element, the strains are more accurate with more element, especially at root. Since the plate element used in this research guarantees the continuity of strains due to bending, i.e., rotation at nodes, the accuracy of sensing may be higher than the brick element that guarantees only displacement continuity at nodes.

Vibration Control of a Laminated Composite Plate

A plate composed of laminated composite whose stacking sequence is $[\pm\theta/0_2]_s$ with piezoelectric S/A pairs shown in Fig. 8 is considered. One side of the plate is fixed and the other sides are free. The sensors are attached over the whole upper surface and the actuators over the lower surface. The S/As can be divided arbitrarily, but must be collocated. The material properties of the Graphite/Epoxy lamina (Hercules AS1/3501-6) and PZT (Clevite Corp.) are shown in Table 1. Twenty-five elements (5 × 5) are used to model the plate and the S/A pair can be attached for each element. Six modes are used in modal space analysis and the feedback gain GG^C is normalized by $1/\bar{z}$.

First, the transient displacements for a plate with 25 S/As are obtained by the direct time integration method. The calculation is performed for $\theta = 90$ deg, with a time step of 0.00025 s. The decay envelopes for feedback gains of 0, 40, and 80 are shown in Figs. 9a and 9b for bending and torsional initial displacements, respectively; the data points are the peak tip displacements in transient response. As the feedback gain increases, the displacements decay faster, with the first torsional mode decaying faster than the first bending mode at the given feedback gain.

Next, the damped frequency and the damping ratio are obtained from complex eigenvalues. To investigate the effect

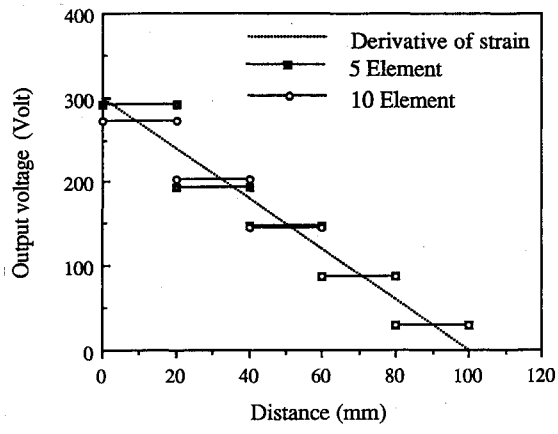

Fig. 7 Convergence of sensor voltage distribution for the bending deflection.

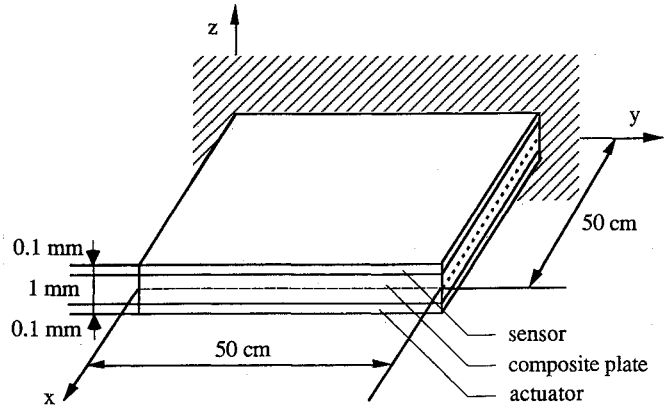

Fig. 8 Laminated plate with piezoelectric sensor/actuator.

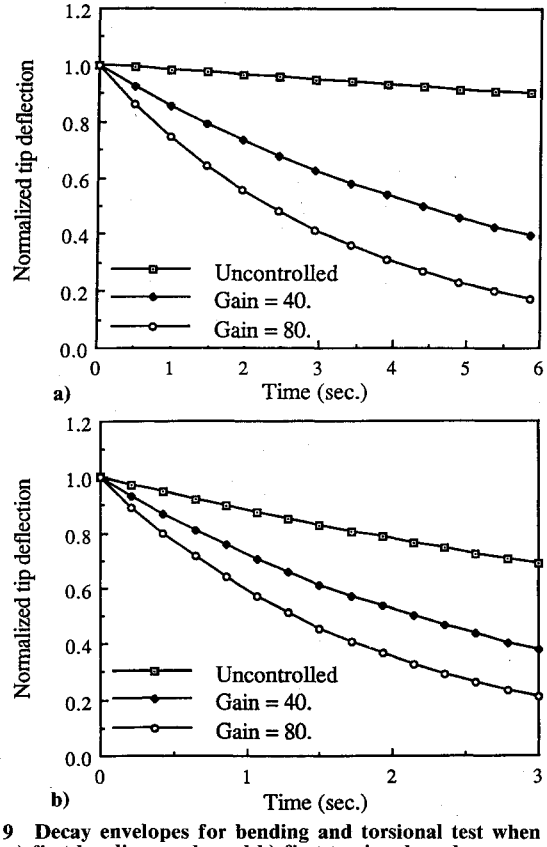

Fig. 9 Decay envelopes for bending and torsional test when $\theta = 90$ deg: a) first bending mode and b) first torsional mode.

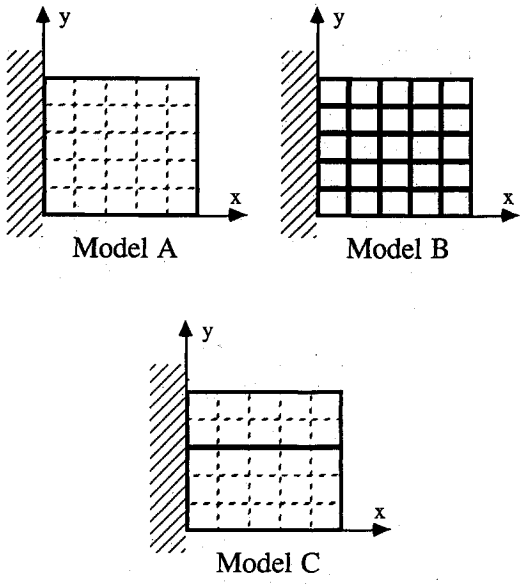

Fig. 10 Models with one sensor/actuator pair (model A), 25 pairs (model B), and two pairs (model C).

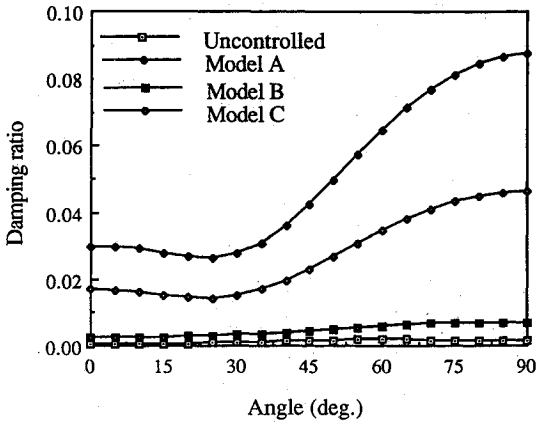

Fig. 11 Damping ratio vs layer angle θ for the first bending mode.

of the division of S/A pairs, model A with one S/A pair, model B with 25 S/A pairs and model C with two S/A pairs over the whole surface are presented in Fig. 10. The simulations are performed for the feedback gain 20 with the varying layer angle θ. The damping ratios for the first bending and torsional modes are shown in Figs. 11 and 12. For the first bending mode, all models show increased damping ratios for any layer angle, with the largest improvement at $\theta = 90$ deg and for model A. For the first torsional mode, model A shows the maximum damping ratio at $\theta = 45$ deg and model B at $\theta = 90$ deg. For model B the damping ratios increase by the same amount regardless of the layer angle; but for model A when $\theta = 0$ deg and 90 deg, the damping ratio is invariant with respect to the feedback gains for the first torsional mode. This is due to the property that a distributed piezoelectric sensor cannot detect the skew-symmetric deformation. One way of overcoming this drawback in model A is to use a composite plate with skewed layer angles of $\theta = 45$ deg, which gives non-skew-symmetric torsional modes and good damping capacities for those modes. Model B with 25 S/A pairs is best at $\theta = 0$ deg and 90 deg, since it shows good damping for the first torsional mode. Since each S/A pair requires one feedback control loop, this increase in the number of the S/A pairs means more control loops are required. Therefore, the design with the minimum number of S/A pairs is preferable. The S/A system with one pair shows good damping capacities, except for its inability to sense skew-symmetric deformation.

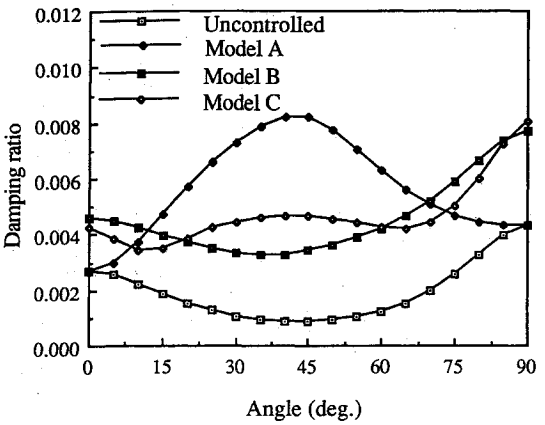

Fig. 12 Damping ratio vs layer angle θ for the first torsional mode.

To overcome this drawback, model C with two S/A pairs was developed. The results for model C in Figs. 11 and 12 show similar damping ratios to model A; however, the drawbacks of model A are overcome at $\theta = 0$ deg and 90 deg. Thus, model C is a mixture of models A and B, making use of the advantage of each system.

Conclusions

An efficient finite element code for vibration control of a laminated composite plate with piezoelectric S/As is developed. A new piezoelectric plate element with one electrical degree of freedom saves memory and computation time compared with previous works. The selective assembling of the element matrices for each electrode and one electrical degree of freedom for an element makes it possible to model and analyze the control systems with the S/As of the various number and geometries of electrodes.

In designing active control systems, the number and the sizes of S/A pairs must be considered as design variables whereas the total area of S/A systems are same. By proper design of distributed S/As, an efficient active control system can be designed for a specified layer angle. Under the same active control system, the damping capacities can be improved by changing the layer angle. This is the mixed effect of changing stiffness, structural damping, and vibration modes.

Since the active control and passive control affect each other, active and passive controls should be considered simultaneously in designing efficient controlled structures. The finite element code developed in this paper is an efficient analysis tool which can accompany S/A design and structural modification.

Appendix: Modal Structural Damping

The damping in composite materials plays an important role in the dynamic problem. Composite materials show high damping in the transverse direction but low in the fiber direction, due to the properties of the polymer and the fibers. The damping property should be considered with respect to layer angle changes, because the damping has a character of orthogonality. The specific damping capacity (SDC) is defined as[23]

$$\varphi = \frac{\Delta U}{U} \tag{A1}$$

where ΔU is the energy dissipated during a stress cycle and U the maximum strain energy. The total dissipated energy is derived in the same way as U,

$$\Delta U = \frac{1}{2} \int_A \kappa^T \boldsymbol{D}^{\Delta} \kappa \, dA \tag{A2}$$

where

$$D_{ij}^{\Delta} = \frac{1}{3} \sum_{k=1}^{N} (\bar{Q}_{ij}^{\Delta})_k (z_k^3 - z_{k-1}^3) \tag{A3}$$

$$\bar{Q}^{\Delta} = P^{-1} \text{ diag } \{\varphi_1 \ \varphi_2 \ \varphi_{12}\} QP \tag{A4}$$

and φ_1, φ_2, and φ_{12} are the damping capacities in the fiber direction, transverse direction, and shear direction, respectively. If ΔU is discretized by Eq. (26) and expressed in nodal variables as U, the SDC can be rewritten as

$$\varphi = \frac{r^T K_D r}{r^T K_S r} \tag{A5}$$

where

$$K_D = \sum_{\text{elem}} \int_A \Psi_\kappa^T D^{\Delta} \Psi_\kappa \, dA \tag{A6}$$

that is, the damped stiffness matrix. The SDC can be derived for each vibration mode, which is called the modal SDC. When the ith mode shape $\{\phi\}_i$ derived in an undamped free vibration is replaced by r in Eq. (A5), the ith modal SDC can be obtained. The modal damping matrix C_{mod} can be derived from the modal SDC as follows:

$$C_{\text{mod}} = \text{diag } \{2\zeta_1\omega_1 \ \ldots \ 2\zeta_2\omega_2 \ldots 2\zeta_n\omega_n\} \tag{A7}$$

where

$$2\zeta_i = \varphi_i / 2\pi \tag{A8}$$

References

[1]Atluri, S. N., and Amos, A. K., *Large Space Structures: Dynamics and Control,* Springer-Verlag, Berlin, 1988.

[2]Wada, B. K., Fanson, J. L., and Crawley, E. F., "Adaptive Structures," *Adaptive Structures,* edited by B. K. Wada, American Society of Mechanical Engineers, New York, 1989, pp. 1–8.

[3]Rogers, C. A., "Intelligent Material Systems and Structures," *U.S.-Japan Workshop on Smart/Intelligent Materials and Systems,* Technomic, Lancaster, PA, 1990, pp. 11–33.

[4]Bailey, T., and Hubbard, J. E., Jr., "Distributed Piezoelectric Polymer Active Vibration Control of a Cantilever Beam," *Journal of Guidance, Control, and Dynamics,* Vol. 8, No. 5, 1985, pp. 606–610.

[5]Plump, J. M., Hubbard, J. E., Jr., and Bailey, T., "Nonlinear Control of a Distributed System: Simulation and Experimental Results," *Journal of Dynamic Systems, Measurement, and Control,* Vol. 109, June, 1987, pp. 133–139.

[6]Crawley, E. F., and de Luis, J., "Use of Piezoelectric Actuators as Elements of Intelligent Structures," *AIAA Journal,* Vol. 25, No. 10, 1987, pp. 1373–1385.

[7]Fanson, J. L., and Caughey, T. K., "Positive Position Feedback Control for Large Space Structures," *Proceedings of the AIAA/ASME/ASCE/AHS 28th Structures, Structural Dynamics and Materials Conference* (Monterey, CA), AIAA, New York, 1987 (AIAA Paper 87-0902).

[8]Hanagud, S., Obal, M. W., and Calise, A. J., "Optimal Vibration Control by the Use of Piezoelectric Sensors and Actuators," *Proceedings of the AIAA/ASME/ASCE/AHS 28th Structures, Structural Dynamics and Materials Conference* (Monterey, CA), AIAA, New York, 1987 (AIAA Paper 87-0959).

[9]Crawley, E. F., and Lazarus, K. B., "Induced Strain Actuation of Isotropic and Anisotropic Plates," *AIAA Journal,* Vol. 29, No. 6, 1991, pp. 944–951.

[10]Wang, B. T., and Rogers, C. A., "Laminate Plate Theory for Spatially Distributed Induced Strain Actuators," *Journal of Composite Materials,* Vol. 25, April 1991, pp. 433–452.

[11]Lee, C.-K., "Piezoelectric Laminates for Torsional and Bending Control: Theory and Experiments," Ph.D. Dissertation, Cornell Univ., Ithaca, NY, May 1987.

[12]Lee, C.-K., O'Sullivan, T. C., and Chiang, W.-W., "Piezoelectric Strain Sensor and Actuator Designs for Active Vibration Control," *Proceedings of the AIAA/ASME/ASCE/AHS 32nd Structures, Structural Dynamics and Materials Conference,* AIAA, Washington, DC, 1991 (AIAA Paper 91-1064).

[13]Schmit, L. A., and Farshi, B., "Optimum Laminate Design for Strength and Stiffness," *International Journal for Numerical Methods in Engineering,* Vol. 7, 1973, pp. 519–536.

[14]Haftka, R. T., Gurdal, G., and Kamat, M. P., *Elements of Structural Optimization,* Kluwer Academic, Dordrecht, The Netherlands, pp. 341–384, 1990.

[15]Tseng, C.-I., "Electromechanical Dynamics of a Coupled Piezoelectric/Mechanical System Applied to Vibration Control and Distributed Sensing," Ph.D. Dissertation, Univ. of Kentucky, Lexington, KY, July, 1989.

[16]Tzou, H. S., and Tseng, C.-I., "Distributed Vibration Control and Identification of Coupled Elastic/Piezoelectric Systems: Finite Element Formulation and Application," *Mechanical Systems and Signal Processing,* Vol. 5, No. 3, 1991, pp. 215–231.

[17]Ha, S. K., Keilers, C., and Chang, F. K., "Finite Element Analysis of Composite Structures Containing Distributed Piezoelectric Sensors and Actuators," *AIAA Journal,* Vol. 30, No. 3, 1992, pp. 772–780.

[18]Jones, R. M., *Mechanics of Composite Materials,* Scripta, Washington, DC, 1975, pp. 147–187.

[19]Parton, V. Z., and Kudryavtsev, B. A., *Electromagnetoelasticity Piezoelectrics and Electrically Conductive Solids,* Gordon and Breach, Amsterdam, The Netherlands, 1988.

[20]Batoz, J.-L., and Tahar, M. B., "Evaluation of a New Quadrilateral Thin Plate Bending Element," *International Journal for Numerical Methods in Engineering,* Vol. 18, 1982, pp. 1655–1677.

[21]Becker, E. B., Carey, G. F., and Oden, J. T., *Finite Elements,* Prentice-Hall, Englewood Cliffs, NJ, 1981.

[22]D'Souza, A. F., and Garg, V. K., *Advanced Dynamics,* Prentice Hall, Englewood Cliffs, NJ, 1984, pp. 198–232.

[23]Lin, D. X., Ni, R. G., and Adams, R. D., "Prediction and Measurement of the Vibrational Damping Parameters of Carbon and Glass Fiber-Reinforced Plastic Plates," *Journal of Composite Materials,* Vol. 18, March 1984, pp. 132–152.